ELSEVIER

Journal of Contaminant Hydrology 43 (2000) 63–90

JOURNAL OF Contaminant Hydrology

www.elsevier.com/locate/jconhyd

Flow dynamics and potential for biodegradation of organic contaminants in fractured rock vadose zones

J.T. Geller [a,*], H.-Y. Holman [a], G. Su [a,b], M.E. Conrad [a], K. Pruess [a], J.C. Hunter-Cevera [a]

[a] *Earth Sciences Division, E.O. Lawrence Berkeley National Laboratory, University of California, 1 Cyclotron Road, MS90-1116, Berkeley, CA 94720, USA*

[b] *Department of Civil Engineering, University of California, Berkeley, CA 94720, USA*

Received 8 January 1999; received in revised form 21 September 1999; accepted 18 October 1999

Abstract

We present an experimental approach for investigating the potential for bioremediation of volatile organic compounds (VOCs) in fractured rock vadose zones. The experimental work was performed with rock samples and indigenous microorganisms from the site of the United States Department of Energy's Idaho National Engineering and Environmental Laboratory (INEEL), located in a basalt flow basin where VOC contamination threatens the Snake River Aquifer. Our approach has four components: (1) establishing a conceptual model for fluid and contaminant distribution in the geologic matrix of interest; (2) identification of important features of liquid distribution by means of seepage experiments in the fracture plane; (3) identification of the presence and activity of microorganisms by non-destructive monitoring of biotransformations on rock surfaces at the micron-scale; and (4) integration of flow and biological activity in natural rock ''geocosms''. Geocosms are core-scale flow cells that incorporate some aspects of natural conditions, such as liquid seepage in the fracture plane and moisture content. Fluid flow and distribution within fracture networks may be a significant factor in the ability of microorganisms to degrade VOCs, as they affect the availability of substrate, moisture and nutrients. Flow visualization and tracer breakthrough curves in transparent fracture replicas for unsaturated inlet conditions exhibited the channelized and intermittent nature of liquid seepage. The seepage of water and non-aqueous phase liquids (NAPLs) of varying physical and chemical properties into an

* Corresponding author. Fax: +1-510-486-7079.
E-mail address: jtgeller@lbl.gov (J.T. Geller).

PII: S0169-7722(99)00095-9

initially dry replica showed only subtle differences in liquid distribution. In contrast, the seepage of a NAPL into the fracture replica containing residual water resulted in complex trapping of NAPL along the solid/water/air contact lines and diversion of NAPL to previously dry parts of the fracture. We found that a mixed culture of viable bacteria exists on the natural rock surfaces. Microbial activity measurably changed in response to changing relative humidity (RH). Biological activity in the geocosm produced changes in liquid surface tension and seepage patterns over time.

Keywords: Unsaturated zone; Fractures; Biodegradation; Volatile organic compounds; Non-aqueous phase liquids; Multiphase flow

1. Introduction

Subsurface contamination from volatile organic compounds (VOCs) is ubiquitous due to the widespread production and use of organic solvents and hydrocarbon fuels. At ambient pressures and temperatures in the shallow subsurface, these substances are commonly introduced into the ground as liquids that are immiscible with water; hence, they are commonly designated as non-aqueous phase liquids (NAPLs) (Mercer and Cohen, 1990).

In arid sites with deep water tables, a significant fraction of near-surface NAPL spills may be contained within the vadose zone. At such sites, NAPL fate above the water table may determine the extent of groundwater contamination. Relatively small volumes of a NAPL can migrate over large distances, both vertically (due to preferential flow paths through channels within fracture planes) and laterally, where vertical fractures intersect horizontal fractures or changing lithology (Roberts et al., 1982; Kueper and McWhorter, 1996). NAPLs may pond at these discontinuities, forming lenses of considerable contaminant mass. Two- and three-phase fluid mixtures may be present within the fractures, including NAPL–gas, water–gas, NAPL–water (in regions of perched water) and NAPL–water–gas. Over time, VOCs partition from the NAPL into the surrounding solid, aqueous and vapor phases (Schwille, 1988; Parker et al., 1994). VOC transport in the aqueous and vapor phases produces extensive lateral and vertical spreading of the contaminant beyond the original NAPL distribution (e.g. Seely et al., 1994; Conant et al., 1996; Johnson and Kueper, 1996; Mendoza et al., 1996). Significant inventories of VOCs may partition and diffuse into the pore space of the less-accessible matrix rock (Parker et al., 1996), where removal by flushing or vapor extraction is seriously limited by slow diffusion processes.

Biotransformation of VOCs in the vadose zone represents both an attractive enhancement (Hoeppel et al., 1991) of, and alternative to, vapor extraction. In a wide variety of subsurface environments, in situ bioremediation has been demonstrated to effectively contain the spread of contaminants (including many chlorinated solvents) while converting a significant fraction of their mass to harmless byproducts (National Research Council, 1994). However, the nature and extent of these processes in the vadose zone and/or fractured rock are not well-understood. There is some field evidence that biodegradation of chlorinated solvents can occur in fractured rock vadose zone settings

(e.g., Conrad et al., 1997b), but major questions remain as to how to characterize the extent of naturally occurring biological activity and how to stimulate and monitor it for the remediation of contaminated aquifers. While the numbers of indigenous bacteria in the fractured rock vadose zone in arid regions are low, experiments have indicated that their activity may be stimulated with the addition of water, nutrients and organic carbon (Palumbo et al., 1994).

We present an approach to determine the potential for bioremediation of VOCs in fractured rock vadose zones in a manner that incorporates the specific geology, liquid seepage patterns and the indigenous microorganisms at a given site. A key aspect of this work is to consider the close coupling between fluid flow dynamics and biotransformation processes. Fluid flow and distribution within fracture networks may be a significant factor in the ability of microorganisms to degrade VOCs, as they affect the availability of substrate, moisture and nutrients. Biological activity can change liquid surface tension and generate biofilms that may change the wettability of solid surfaces, locally alter fracture permeability and redirect infiltrating liquids.

This paper is organized around the four components of our approach: (1) establishing a conceptual model for fluid and contaminant distribution in the geologic matrix of interest; (2) experiments of liquid seepage in the fracture plane; (3) non-destructive monitoring of biotransformations on rock surfaces at the micron-scale; and (4) integration of flow and biological activity in natural rock ''geocosms''. Geocosms are core-scale flow cells that incorporate some aspects of natural conditions, such as liquid seepage in the fracture plane and moisture content. The experimental work was performed with rock samples and indigenous microorganisms from the site of the United States Department of Energy's (USDOE) Idaho National Engineering and Environmental Laboratory (INEEL), located in a basalt flow basin where VOC contamination threatens the Snake River Aquifer.

2. Geologic matrix and fluid distribution

The conceptual model for fluid and contaminant distribution begins with an understanding of the geologic matrix. The INEEL is located in the Eastern Snake River Plain (ESRP) which was formed from sequences of basalt flows. The flows are often bounded by rubble zones and sedimentary interbeds of clay, silt, sand and gravel that may accumulate between flow events. A typical basalt flow can extend over an area of 150–300 km^2 (Whitehead, 1992), with individual lobes extending 300 m in length, 30–120 m in width and from 3 to 10 m thick, overlapping and building on the undulating topography of previous flows (Knutson et al., 1990; Sorenson et al., 1996). Perched water often occurs at the sedimentary interbeds between the basalt flows. Most of the groundwater recharge arises from spring melt of the surrounding mountain snowpack, part of which is transported across the surface of the ESRP by ephemeral rivers. A comprehensive geologic description of the basalt flows of the ESRP is presented by Whitehead (1992).

The cooling behavior of the basalt flow produces layers of different textures within a given flow unit. The bottom layer is usually fractured and rubbled, and is overlain by a

vesicular element, generally fractured into columnar polygons. Above the lower vesicular element is a coarse-grained, massive, generally non-vesicular central element, which comprises about half of the flow thickness, and is generally quite dense with few fractures except for vertical columnar joints. The upper vesicular element typically accounts for about a third of the total flow thickness. This element may have a parting parallel to the upper surface as well as fissures and broken basalt that may contribute to rubble zones in the substratum of the overlying flow (Knutson et al., 1990). The upper portion of the flow unit, or entablature, generally consists of columns of smaller diameter, formed by the rapid convective cooling near the surface, relative to the more widely spaced columns of the lower portion of the basalt flow, called the colonnade, which formed from slower conductive cooling (Degraff and Aydin, 1993; Degraff et al., 1989; Long et al., 1995). The column bounding fractures of the colonnade and entablature may intersect, may terminate within the rock matrix, or may be connected laterally by column-normal fractures (Long et al., 1995).

While regional, lateral groundwater transport is controlled by the large-scale layering of multiple basalt flows and rubble zones (Sorensen et al., 1996), processes affecting contaminant fate are also controlled by smaller-scale features within a given basalt flow or a vertical sequence of a few layers. The vesicular basalt matrix rock has large storativity, but low hydraulic conductivity, arising from the poorly connected trapped bubbles formed when the basalt cooled. While liquid seepage occurs mostly in the fractures, and through rubble zones, seeping liquids can accumulate and slowly imbibe into the matrix rock where fractures intersect horizontal discontinuities (including perched water) or terminate within the matrix (Faybishenko et al., 1999). The lower permeability of the dense basalt implies that most of the fluid phase remains in the fractures. Fracture geometry will also affect NAPL distribution and fate. Core examination from slanted holes at Box Canyon, an uncontaminated site adjacent to the INEEL, revealed vertical fractures with smooth, parallel sides, consistent with cooling cracks. The horizontal fractures frequently have rougher and more non-parallel walls and may intersect vesicles (Long et al., 1995); NAPL trapping in these fractures is likely to be much more significant than in vertical fractures due to their greater roughness and small gravity component for flow.

While the pore space of the vadose zone is only partially saturated with water, the relative humidity (RH) of the air should be close to 100% several meters below the ground surface. This is because it takes extremely high suction pressures (i.e., very dry rock) to reduce water vapor pressure significantly below saturated values. For example, a large number of in situ measurements in the very thick unsaturated zone at Yucca Mountain, Nevada, have shown moisture tension (= suction pressure) in the range from -0.3 to -0.6 MPa (Rousseau et al., 1997). At 20°C, the average temperature in the deep vadose zone, the Kelvin equation (e.g., Adamson, 1980), predicts a RH of 99.8% and 99.6% for -0.3 and -0.6 MPa, respectively.

Even in the absence of flowing liquid water, the vapor phase may provide enough water to maintain the viability of microorganisms that may become active during seepage events. In air at 100% RH, vapor condensation can readily occur with small decreases in temperature. Furthermore, osmotic pressure gradients will drive vapor condensation onto a more saline liquid (perhaps microorganisms) at aqueous–gas

interfaces. Therefore, liquid water may occur and be available to microorganisms in regions not directly contacted by seepage water.

3. Isotopic evidence for biodegradation of VOCs in the vadose zone at INEEL

The potential significance of biological activity in contaminated fractured rock vadose zones is indicated by isotopic evidence from the Radioactive Waste Management Complex (RWMC) at the INEEL, where a major plume of VOCs exists in the vadose zone (Lodman et al., 1994). Low-level radioactive waste resulting from USDOE activities was deposited in drums in the shallow pits ($\sim$1.5 m deep) at the RWMC. These drums also contained significant amounts of chlorinated hydrocarbon compounds (e.g., carbon tetrachloride, 1,1,1 trichloroethane, and trichloroethene) mixed with lubricating oils. Vapor samples collected from monitoring wells at the site contain high levels of chloroform, which is an intermediary byproduct of biodegradation of carbon tetrachloride, but is not an original component of the waste.

Based on this evidence of biodegradation of the contaminants, a study of the amounts and carbon isotopic compositions of CO_2 in the subsurface was conducted (Conrad et al., 1997b). Many biological reactions preferentially utilize the lighter isotopes, causing the isotopic compositions of the substrates and the products to be shifted from their original ratios. CO_2 concentrations in gas samples collected from two background wells located approximately 1 km southeast of the complex ranged from 0.04% to 0.2% by volume, with the highest concentrations in shallower samples. In the vicinity of the disposal pits, CO_2 concentrations were significantly higher (up to 2%) in the subsurface. The values of the carbon isotope ratio ($\delta^{13}C$) of the CO_2 in the background wells were between $-13‰$ and $-21‰$ and generally decreased with increasing depth. In the complex, the $\delta^{13}C$ values were somewhat lower, ranging between $-18‰$ and $-23‰$, with the lowest values occurring in the samples with the highest CO_2 concentrations. The lower $\delta^{13}C$ values of the enriched CO_2 samples suggest a depleted ^{13}C source, such as the chlorinated hydrocarbon compounds or lubricating oil. In the background wells, the radiocarbon concentrations of CO_2 were near modern atmospheric concentrations. In the contaminated area, the ^{14}C content of the CO_2 ranged from 0 to greater than 100 times modern concentrations. The high ^{14}C CO_2 is derived from radioactive waste with elevated ^{14}C (cement blocks used to shield nuclear reactors) that was deposited at the RWMC. The CO_2 with less than modern levels of ^{14}C, however, was undoubtedly a byproduct of biodegradation of hydrocarbon compounds such as the chlorinated compounds and/or the lubricating oils that were manufactured from fossil fuels (Conrad et al., 1997a).

These data (increased chloroform, increased CO_2, shifts in the isotopic compositions of the CO_2) provide strong evidence that some biodegradation of the contaminants is occurring in the vadose zone at the RWMC. Whether the degradation is occurring in the immediate vicinity of the waste, possibly in an anaerobic pocket beneath the pits, in regions of perched water, or throughout the vadose zone is not evident from the data. It is also not obvious if all the contaminants are being degraded or which degradation pathways (aerobic or anaerobic) are important. Without answering these and other

questions, it will be difficult to predict the ability of the natural biological activity to contain the plume or to design a program to enhance bioremediation at the site.

4. Experimental investigations

The experiments presented here investigate liquid seepage phenomena in single fracture and biotransformation processes on natural rock surfaces. The understanding gained from these experiments is then integrated in an experiment of water seepage within a fracture plane in the presence of microorganisms. This link is based upon our hypothesis that liquid distributions and flow patterns within the fracture plane set the stage for potential biotransformations, as they affect the transport of water, nutrients and contaminants to and from microorganisms.

4.1. Liquid seepage in fractures

We describe flow visualization and tracer experiments of gravity-driven unsaturated flow within a transparent replica of a natural rock fracture that were conducted to identify important flow phenomena and develop conceptual models of liquid seepage in the fracture plane. In flow visualization experiments, liquid is introduced to an inclined fracture replica at slightly negative inlet pressures to maintain partially saturated flow. Experiments are conducted for a range of inlet pressures, angles of inclination and liquid properties. Inlet pressures, flow rates and liquid distribution are continuously monitored. These experiments provide a direct correlation between fracture geometry (i.e., aperture distribution), fracture inclination, liquid properties and seepage behavior. Detailed descriptions of the experiments can be found in Geller et al. (1997, 1998) and Su et al. (1999).

We also perform tracer tests for unsaturated flow to measure the travel time of flowing water through the fracture plane. Travel time is a quantitative measure of preferential flow and an indication of the potential for physical, chemical and biological equilibration between the flowing liquid and the phases it contacts. The interpretation of the tracer breakthrough curves (BTC) is enhanced with flow visualization. This understanding can then be applied to the interpretation of BTCs in natural fractured rock where the liquid distribution cannot be directly observed.

Fig. 1 shows the aperture distribution in a 21.5×33 cm^2 epoxy (Eccobond 27, W.R. Grace, Canyon MA) replica cast from both halves of a natural granite fracture (Su et al., 1999), using a procedure adapted from Gentier (1986) and described by Persoff and Pruess (1995). The aperture distribution of the fracture replica is measured non-destructively from light attenuation through the replica saturated with dyed water (after Persoff and Pruess, 1993, 1995; Nicholl et al., 1994; Glass and Nicholl, 1995). The attenuation of light is a function of the distance the light travels, and is correlated to the width of open space of the fracture by calibration to the intensity of light transmitted through known apertures filled with the same liquids.

The surface properties of the epoxy replica are important in interpreting the results of the following seepage experiments. Water is intermediately wetting to epoxy (contact

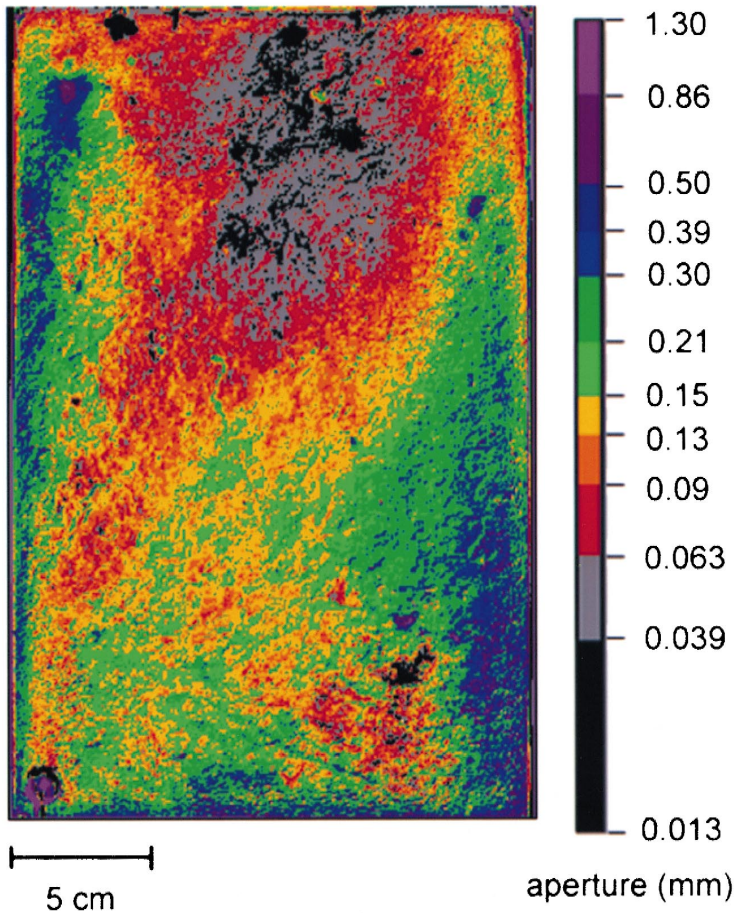

Fig. 1. Aperture map of epoxy replica of natural granite fracture measured from light attenuation (from Su et al., 1999).

angle ranges from 57° to 65°; Geller et al, 1996), which somewhat reduces capillary forces and trapping of the non-wetting phase compared to strongly water-wet systems. Most common aquifer minerals, such as quartz, carbonates and sulfates, are strongly water-wet (Demond and Lindner, 1993); however, natural hydrophobic organic materials and anthropogenic organic compounds on the mineral surface may create conditions of neutral wettability. Powers et al. (1996) found that a wide range of wetting conditions results from the exposure of sands to complex organic liquid contaminant mixtures. Geller et al. (1996) measured a 57° contact angle for water on a smooth, clean granite surface. This is much closer to the contact angle of water on epoxy, than on glass, which is commonly used as an analog for natural rock surfaces (Nicholl et al., 1994). Geller et al. (1996) also observed that a water drop on the fracture surface of the same rock sample spread spontaneously, illustrating the important role that near-surface porosity

and small-scale roughness of a natural fracture surface may have on wetting behavior. An additional consideration in the use of the transparent replicas is that they are non-porous and therefore do not incorporate matrix interaction. Some degree of matrix interaction can be obtained with flow visualization by using one half of the rock fracture mated to a transparent replica of the second half, which is used in the geocosm experiment described towards the end of this paper.

Fig. 2 describes the experimental arrangement for liquid delivery to the fracture, either with constant head (Mariotte bottle) or constant flow (syringe pump) inlet conditions. Water seepage patterns in the replica for constant head inlet conditions are shown in Fig. 3. In this experiment, the replica was inclined at 70° from the horizontal, with -3.5 cm H_2O tension maintained at the inlet. The seepage pattern corresponds to the measured aperture distribution in Fig. 1, with water spreading transverse to the flow direction in the tightest aperture regions, forming ''capillary pools'', while narrow channels form in the larger aperture regions. Water flows in one or two narrow channels that undergo cycles of snapping and reforming, even though pressure is maintained constant at the inlet. This cycle is shown in the enlarged red boxed region. Intermittent flow occurs for a large range of flow conditions, surface properties and angles of fracture inclination. Su et al. (1999) present a detailed laboratory investigation of intermittent flow as a function of fracture aperture distribution, boundary conditions and fracture inclination. We have observed intermittent flow in rock–replica combinations, where a natural rock fracture is mated to a replica of the second half, and in fracture models constructed of parallel glass-plates (Geller et al., 1996, 1997; Su et al., 1999). Under field conditions, unsteady seepage will arise from the episodic nature of recharge events.

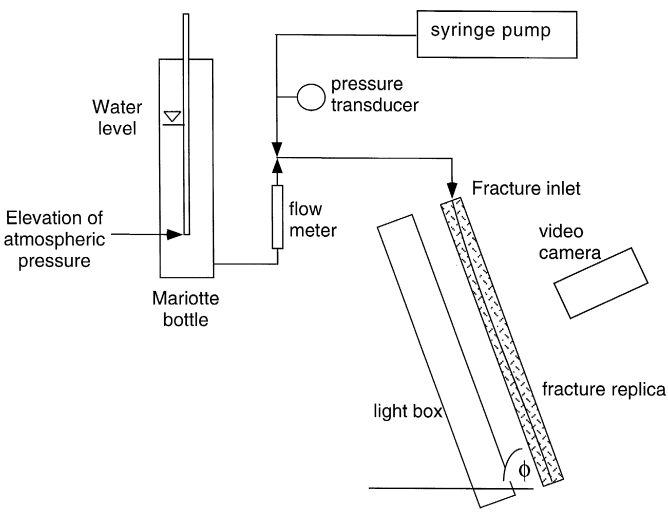

Fig. 2. Water delivery to fracture replica, either by syringe pump for constant flow, or by Mariotte bottle for constant pressure.

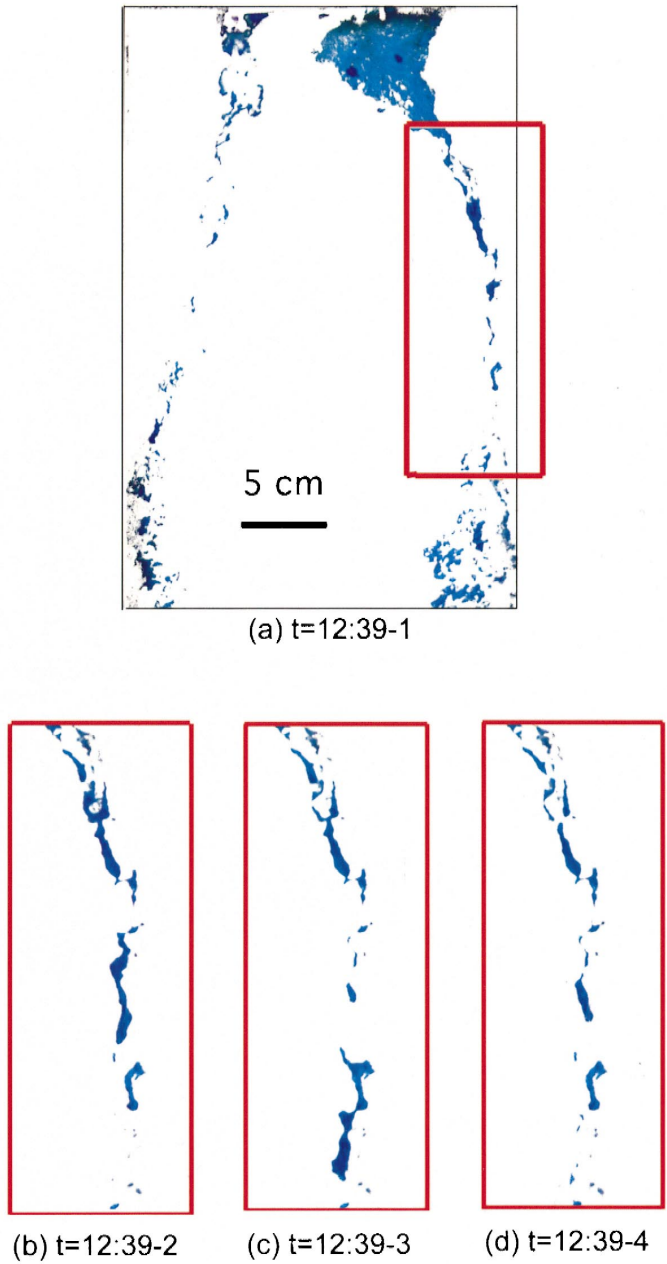

Fig. 3. Water distribution (grey) during percolation, fracture inclined 70° from the horizontal, inlet water tension = −3.5 cm H_2O. Flow channels appear disconnected, but water is flowing through the right channel along narrow rivulets that connect larger liquid-filled regions, as indicated by the change in distribution with time. Images are within seconds of one another. (b)–(d) are enlargements of boxed area in (a).

Tracer breakthrough curves are shown in Fig. 4a and b, for a flow rate of 5 ml/h at a fracture inclination (ϕ) of 81° from the horizontal. The change in the electrical conductance of the liquid, which is directly proportional to tracer concentration, is measured with two pairs of gold wire electrodes embedded in the fracture inlet and outlet for a step input of an electrolyte tracer (4.5×10^{-3} M $CaCl_2$). The results are plotted in terms of the measured concentration C, normalized by the concentration of the introduced tracer C_0. Direct observation showed that the fluctuations in the outlet breakthrough curve (Fig. 4b) correspond to intermittent flow behavior. Fig. 4c plots the travel times from tracer tests at three different angles of inclination and for flow rates of

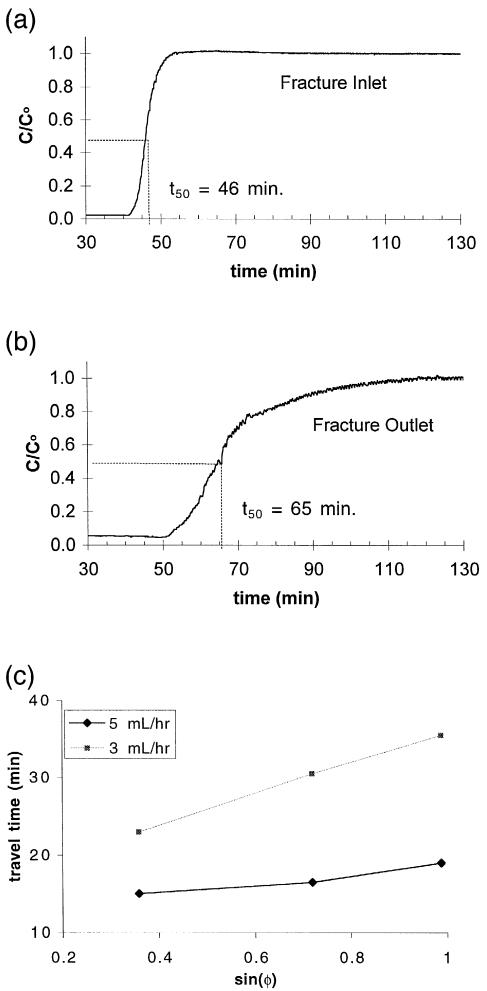

Fig. 4. (a) and (b) Breakthrough curves from tracer test in fracture replica for 5 ml/h, 81° inclination from the horizontal. (a) Fracture inlet. (b) Fracture outlet. (c) Travel time is measured from the difference of the times at $C/C_0 = 0.5$ between the outlet and inlet, as a function of fracture inclination angle (ϕ).

3 and 5 ml/h as a function of gravity force (proportional to sin ϕ). The travel time is calculated from the difference of the fracture outlet and inlet tracer breakthrough times at $C/C_0 = 0.5$. The measured increase in travel time at higher angles seems counterintuitive, but information from flow visualization provides an interpretation of this result. Visual observation showed that the frequency of channel snapping increases at higher angles of inclination, suggesting that flow intermittence increases liquid hold-up in the fracture.

The seepage of liquids of varying physical and chemical properties in an initially dry fracture exhibits subtle differences in behavior. This is shown in Fig. 5, which compares the liquid distribution following seepage into the initially dry fracture replica for water and two NAPLs: *n*-dodecane and PCE. These liquids represent a range of density and viscosity contrasts relative to water (Table 1). While the liquid distributions are similar, the frequency at which the narrow channel below the wide capillary pool snaps and reforms is approximately five times greater for the NAPLs than for water. This is explained by the increased lateral spreading of the NAPLs, which have zero contact angle on the epoxy, compared to the reduced spreading of water. The lateral spreading of the NAPL removes more mass from the flowing channel, which in turn increases the rate at which it thins and subsequently snaps.

In contrast to the behavior of a single liquid phase, the seepage of an NAPL into a fracture with residual water gives rise to even more complex fluid distributions. Fig. 6 shows the liquid distribution after *n*-dodecane (red) was introduced into a fracture

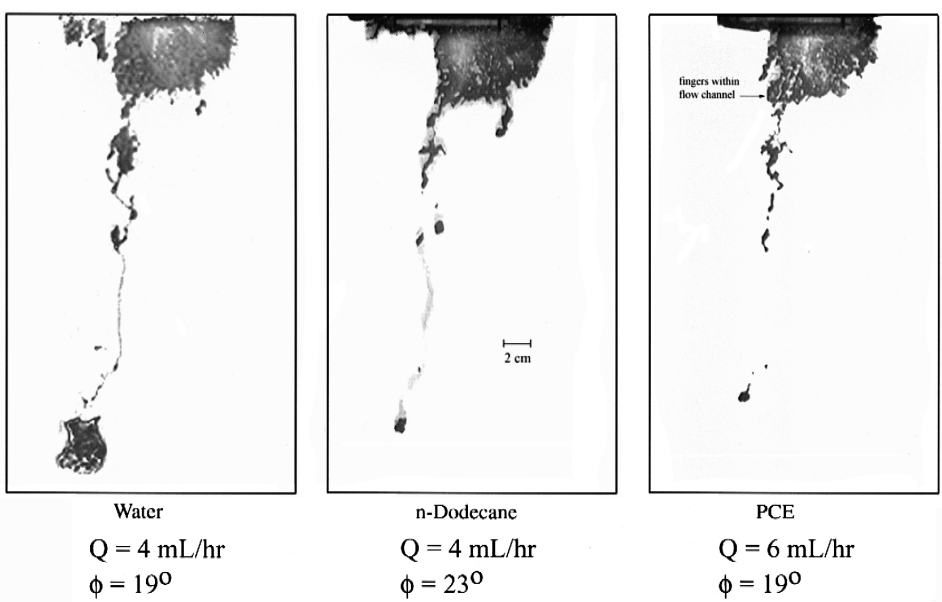

Fig. 5. Liquid distribution during three seepage experiments for water, *n*-dodecane and PCE into the initially dry fracture replica. Grey indicates liquid-occupied regions, white regions are dry. Images were taken immediately before the initial invading finger broke through the fracture outlet.

Table 1
Properties of liquids used in the seepage experiments (at 25°C and atmospheric pressure unless otherwise noted)

Liquid	Density[a] (kg/m^3) (pure liquids)	Viscosity[a] (10^{-3} Pa s) (pure liquids)	Air/liquid surface tension (mN/m) (dyed liquids)[b]	Contact angle on epoxy (°) (pure liquids)	Vapor pressure (mm Hg) (pure liquids)
Water	997[c]	1.10[c]	64.4[d]	62[e]	23.8[c]
n-dodecane	745	1.38	25.2[f]	0[g]	0.12[h]
PCE	1630	0.89	31.2[f]	0[g]	17.8[i]

[a] Riddick and Bunger (1970).
[b] Water dyed with 0.4% Liquitint; NAPLs dyed with 1 mg/l Spectra Oil Red.
[c] Tchobanoglous and Schroeder (1987).
[d] Geller et al. (1996), 21°C.
[e] Measured with goniometer (Ramé-Hart, Mountain Lakes, NJ), 21°C.
[f] Measured with surface tensiometer (model 21, Fischer Scientific), 21°C.
[g] Direct observation.
[h] Mackay and Shin (1974).
[i] Mercer and Cohen (1990).

having residual water (blue) saturation. The NAPL flows along solid/water/air contact lines and is also diverted by the presence of residual water to dry parts of the fracture, resulting in a more dispersed distribution than in an initially dry fracture. NAPL trapping occurs both along the water–air interface and in the previously dry parts of the fracture. Observation of subsequent water infiltration further complicates the distribution of liquid–liquid–vapor interfaces due to additional water trapping along NAPL–air interfaces.

High-resolution numerical simulations of liquid seepage in heterogeneous fractures performed with conventional finite difference methods have been described by Pruess (1998, 1999). These have produced many of the characteristics observed in laboratory experiments and field systems, including localized preferential flow, ponding, and bypassing (Pruess, 1998, 1999). However, no flow intermittence was seen in the numerical simulations, which may indicate limitations of the continuum approach used.

4.2. Biotransformation of volatile organic contaminants in naturally fractured rock

Laboratory characterization of biotransformation processes in a manner that represents natural field conditions is a major challenge. The activity of microorganisms attached to a solid differs greatly from planktonic microorganisms, in terms of their resistance to toxic chemicals and the transport of contaminants and nutrients to the microorganism. This is, in part, due to the production of exopolysaccharides (EPS) upon attachment, and formation of ''organized communities'' or biofilms (Marshall, 1985; Costerson, 1995). This limits the relevance of traditional batch reactor tests of suspended media in determining the potential for biotransformation of contaminants. Prevailing subsurface conditions of constant near 100% RH are difficult to replicate in the laboratory. Another challenge is the study of reactions at the dilute environmental

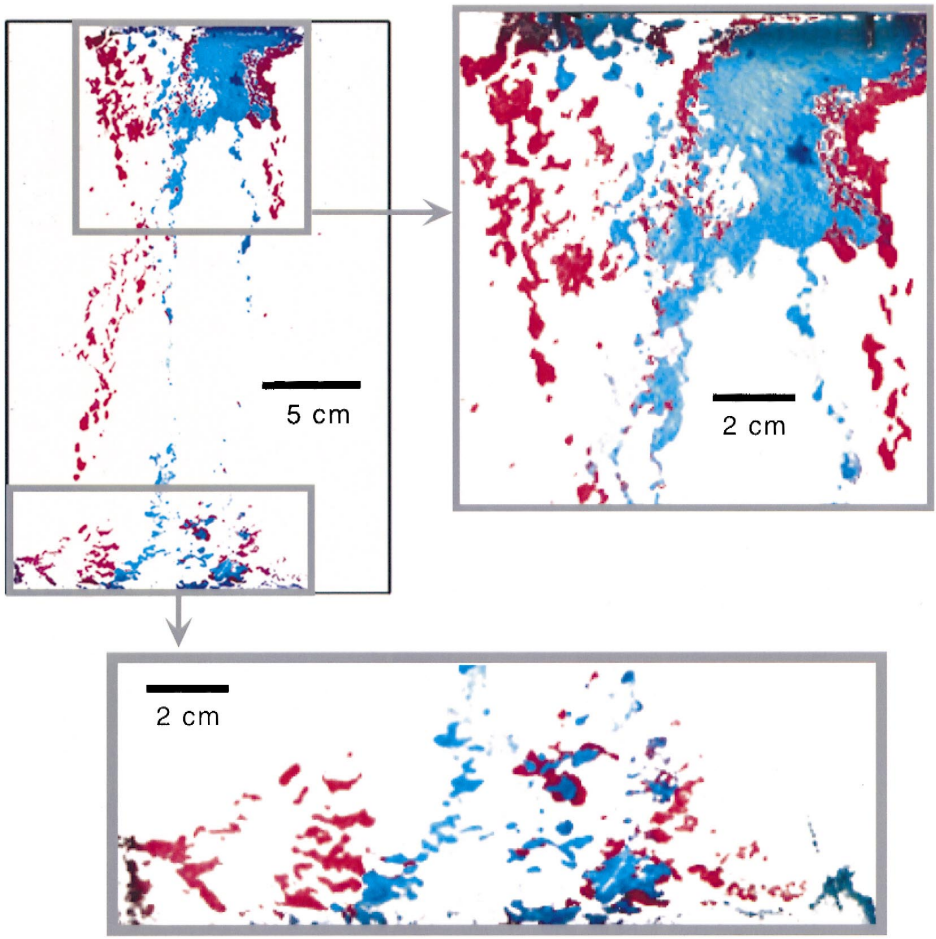

Fig. 6. Distribution of NAPL (dodecane, dyed red) introduced into fracture replica containing residual water (dyed blue). Enlarged sections show NAPL trapping along air/water/solid contacts.

concentrations of microorganisms and chemical species that occur in the fractured rock vadose zone.

Significant issues arise in obtaining samples of indigenous microorganisms associated with subsurface geologic materials. We acquired core samples from the vadose zone at the Test Area North (TAN) site at INEEL within the context of the Department of Energy's Subsurface Science Program. These samples were obtained according to the protocol developed by Colwell et al. (1992), whereby the extent of contamination of non-indigenous microorganisms is determined, and an undisturbed ''defensible'' sample can be subsampled from the core. Drilling fluid is expected to contact fracture surfaces during sampling, and therefore, defensible samples of fractures themselves cannot be obtained. The samples were acquired within a 10-ft interval above the current groundwa-

ter table, where aqueous concentrations of trichloroethylene were on the order of 1 ppm. In this location, it was hoped that the indigenous microorganisms had acclimated to the presence of organic contamination.

Our approach, based on the above considerations, is to characterize indigenous microorganisms and evaluate the potential for contaminant degradation on defensible samples in microscale experiments. Then, column-scale studies, termed ''geocosms'', are conducted on sterilized basalt rock inoculated with culturable organisms extracted from the defensible samples. In geocosms, we consider the mass transfer limitations to biological activity arising from fluid distribution. The experimental work described in Sections 4.2.1 and 4.2.2 lays the groundwork for studies involving actual contaminant degradation.

4.2.1. Micro-scale experiments

We have developed and applied two innovative techniques at Lawrence Berkeley National Laboratory's Advanced Light Source Facility to monitor the space and time-resolved biological activity and chemical transformations on mineral surfaces. These measurements provide a 10-μm spatial resolution of bacterial, mineral and contaminant distribution on the surfaces of natural and treated geologic media, and have provided mechanistic insights regarding biological activity on mineral surfaces.

In the first technique (Holman et al., 1998a), surface-enhanced infrared reflectance absorption (SEIRA) microspectroscopy was applied to qualitatively monitor the in situ localization of microorganisms on mineral surfaces and relate the distribution to the microstructure and mineral composition of the rocks. A photograph of a section of the ''defensible'' intact basalt core obtained from INEEL is shown in Fig. 7A. It is an iron–magnesium-rich rock, consisting mainly of calcic plagioclase feldspar, pyroxene

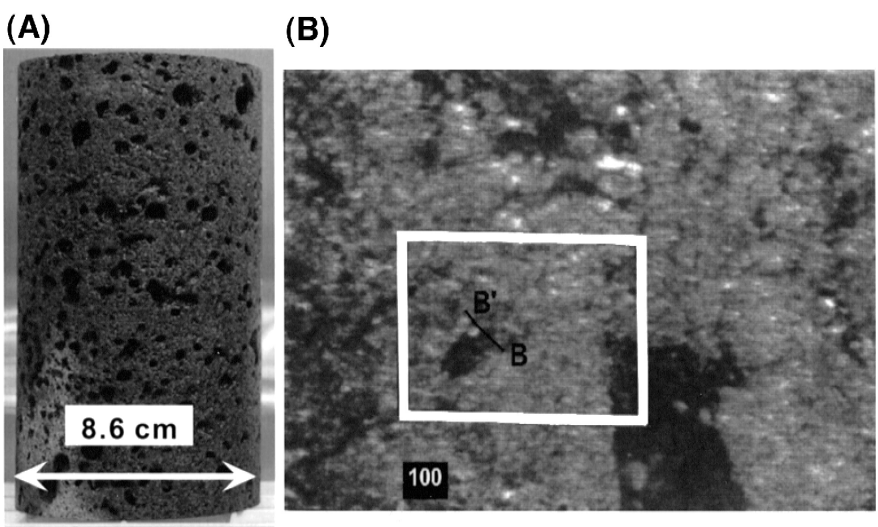

Fig. 7. (A) The 8.6-cm diameter core sample from INEEL; (B) microphotography of the $400 \times 500\ \mu m^2$ study area. Axis BB′ is the sampling path for Fig. 13. The two prominent dark areas are two vesicles in the basalt specimen.

and olivine. Vesicles occupy about 10–25% of the bulk volume. Some vesicles have secondary mineral coatings. Cores such as these were sliced aseptically by a specially modified tool from which subsamples for microscale studies were selected. Fig. 7B is a photomicrograph of the $400 \times 500\ \mu m^2$ area used in this study.

Six isolates were identified from cultivable colonies sampled from the vesicle surfaces of the defensible samples using fatty acid methyl ester (FAME) analysis. Two isolates were Gram-negative (*Pseudomonas putida* and *P. fluorescens*) and four were Gram-positive (*Arthrobacter oxydans*, *Bacillus atrospecticus*, *Micrococcus lylae* and *Nocardia globerula*). Similar bacteria have been found in other terrestrial deep subsurface environments (Haldeman et al., 1993; Zheng and Kellogg, 1994; Amy, 1997; Balkwill and Boone, 1997). From the absorption intensity spectra of these isolates, we identified two absorption peaks as ''biomarkers'' for mapping the distribution of bacteria and changes in their level of activity; the microbial protein Amide I with an absorption peak at 1650 cm^{-1} wave number, and the protein Amide II at the 1550 cm^{-1} wave number. The absorption bands for the biomarkers are distinct from the absorption bands due to the presence of silicate minerals, which occur within the 1300–800 cm^{-1} region.

Areal contour maps of the absorption peak heights over different absorption bands were derived from measurements with a Fourier Transform Infrared (FTIR) spectrometer through a $10 \times 10\ mm^2$ aperture with a computer-controlled x–y mapping stage. Fig. 8a is a contour plot of the relative absorption intensity in the 1300–800 cm^{-1} region for silicate minerals. Zero values coincide with the vesicles indicated in Fig. 7B, and values greater than zero indicate the presence of silicate minerals in arbitrary units that qualitatively indicate their relative amounts. Fig. 8b shows the contour plot of the absorption intensity at 1650 cm^{-1}; the Amide I biomarker coincides with the dark areas that represent vesicles in Figs. 7b and 8a, indicating that bacteria are associated with the vesicle surfaces. The high-absorption intensity contours extend somewhat beyond the vesicle wall, suggesting that bacteria may have bored into the rock matrix from the vesicle surface.

The SEIRA results are consistent with confocal laser scanning microscopy obtained from the same sample before SEIRA was performed. Fig. 9 shows the distribution of microbial colonies along the edge of the central vesicle in the study area, observed with simultaneous excitation at 488 and 514 nm. Independent measurements showed that the above-mentioned isolates fluoresced naturally at these wavelengths. The depths denoted in the images are relative to the base of the brightest colony. This is defined as the point below which fluorescence due to the isolates disappears, which should correspond to the basalt surface. The scans at different focal lengths at other locations on the samples indicate that most of the microbial colonies extend less than 1 μm from the basalt surface.

Higher-resolution scanning was conducted through the bacteria colony clusters along the axis BB′, denoted in Figs. 7 and 9b. Regions A through B in Fig. 10 show a decline in biomarker peaks, which disappear abruptly at the transition into the bacteria-free area indicated by region C (scan no. 24). These scans are more sensitive to the presence of bacteria compared to the confocal laser scanning microscopy, indicating that not all the indigenous bacteria fluoresce at 488 and 514 wavelengths, and that other species, in

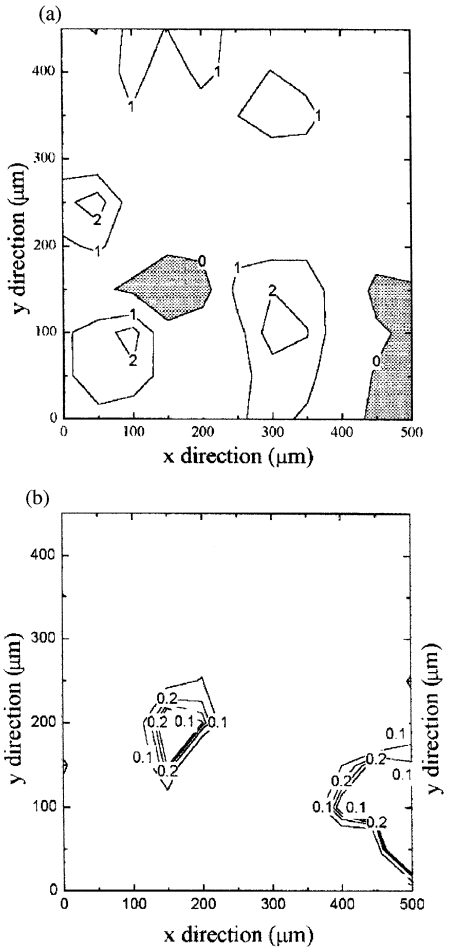

Fig. 8. Contour plots of the study area in Fig. 10b based on absorption intensity of (a) silicate-containing minerals in basalt in the 1300–800 cm^{-1} region, (b) microbial protein Amide I at 1650 cm^{-1}.

addition to those isolated, are present. Dramatic changes in the spectra within the silicate mineral absorption band (1300–800 cm^{-1}), indicated in regions D through F, show that the decline in biomarker peaks corresponds to a change in mineralogy. Specifically, the sharp spectral features in region F are associated with the appearance of calcic plagioclase feldspar, suggesting that bacteria do not attach to this mineral.

The second mapping technique involved the use of a synchrotron infrared beam to non-destructively measure the change in microbial activity on the basalt surface in response to changes in RH. Details of the technique can be found in Holman et al. (1998b, 1999). Toluene degradation by *A. oxydans*, isolated from the defensible samples, was monitored at 100%, then at 25% RH. These large contrasts in RH values compare conditions at depth with conditions that represent near-surface desert soils.

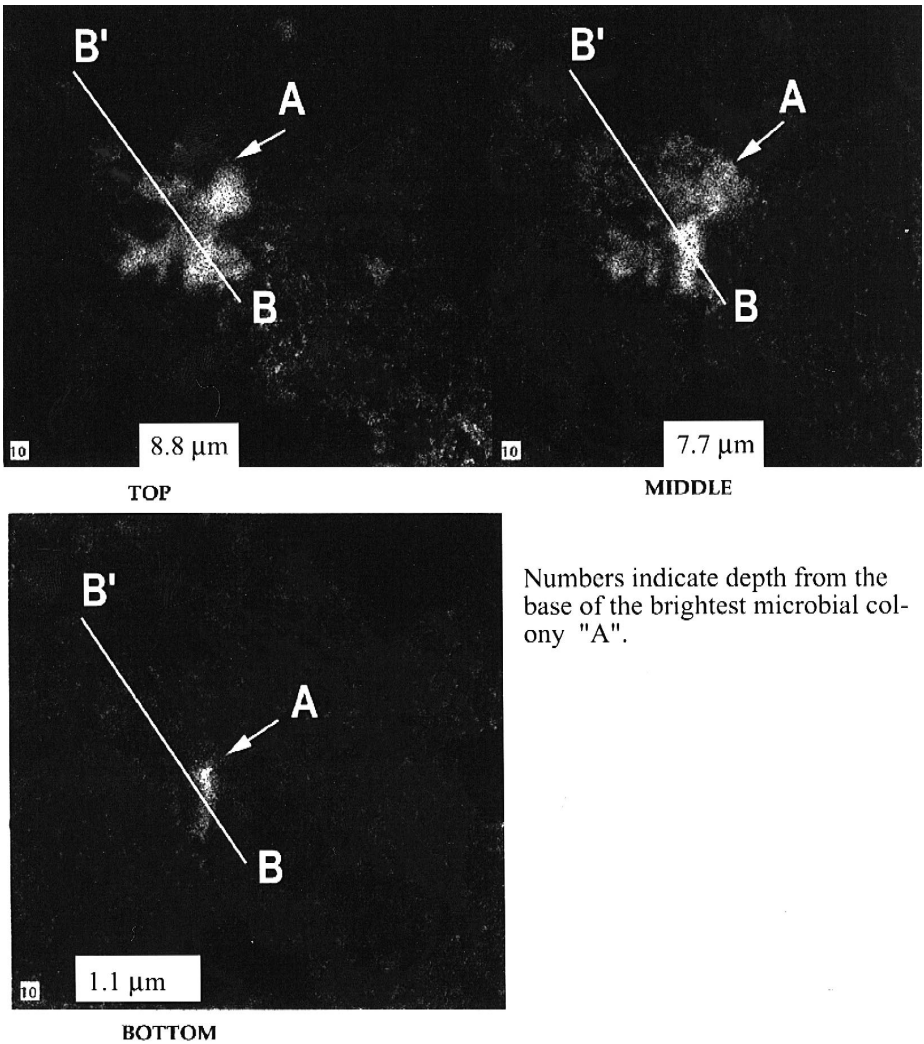

Fig. 9. Confocal fluorescence micrograph of $x-y$ sections showing images of microbial clusters at three different optical depths through the colonies attached to the vesicular basalt sample. The depths denoted in the images are relative to the base of the brightest colony. This is defined as the point below which fluorescence due to the isolates disappears, which should correspond to the basalt surface. The microbes were observed with simultaneous excitation at 488 and 514 nm. Axis BB′ is the same sampling path shown in the microphotograph in Fig. 7B.

Small RH changes of less than 1% have been shown to significantly affect biofilm morphology and toluene utilization (Holden et al., 1997). Toluene was chosen for this first experiment because it is known to be readily degradable and has stable, known metabolites. The results are plotted in terms of the relative intensity peaks for the biomarker protein Amide I ($\sim 1670\ cm^{-1}$), toluene ($728\ cm^{-1}$), and its early metabo-

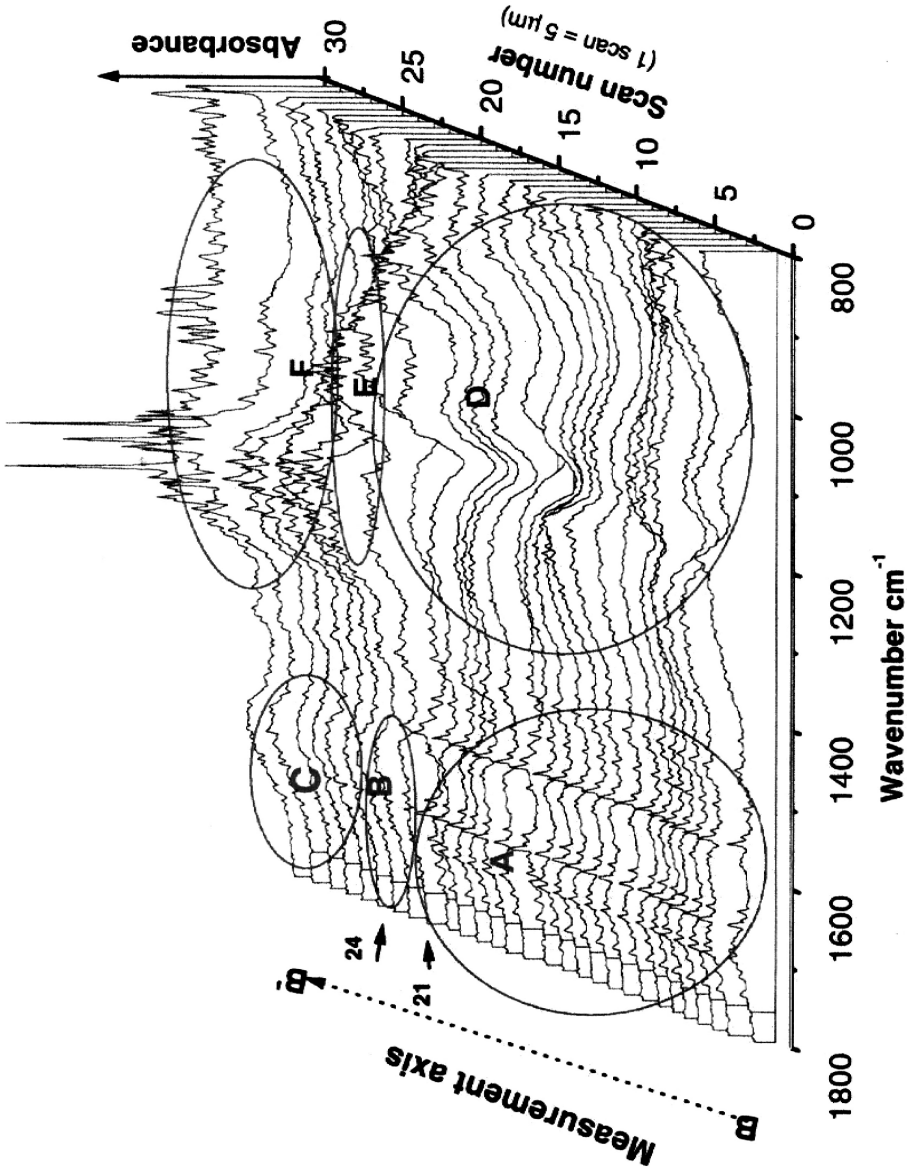
Absorbance
Scan number
(1 scan = 5 μm)
Wavenumber cm-1
Measurement axis
A
B
C
D
E
F
24
21

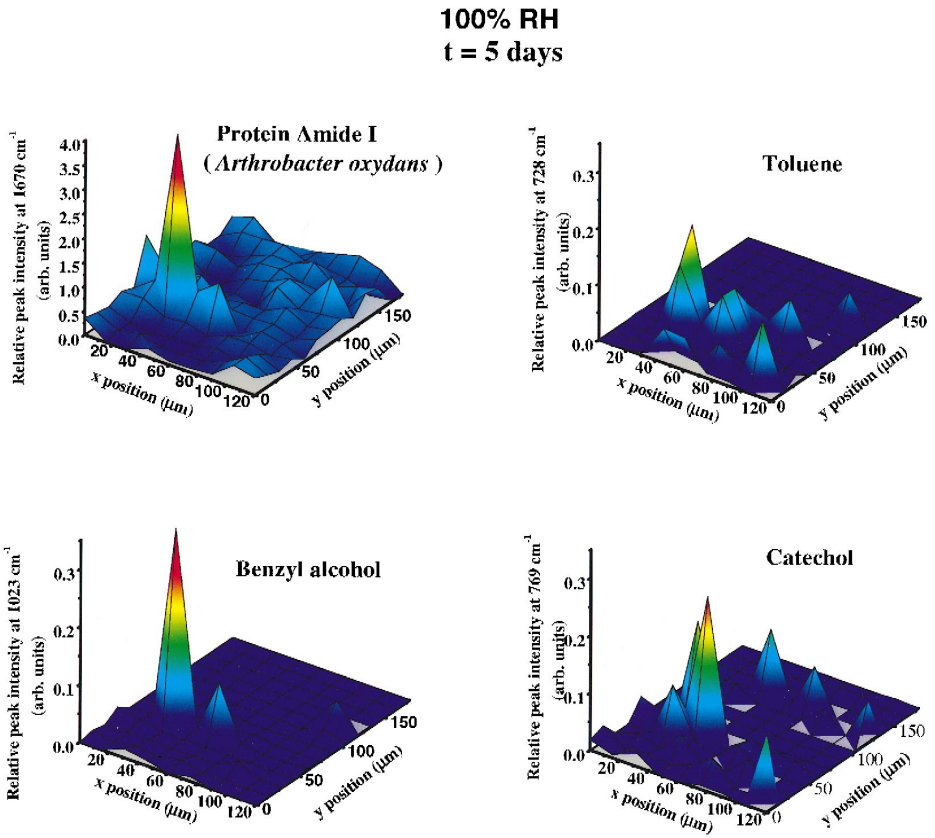

Fig. 11. *A. oxydans* bacteria, isolated from our rock sample, re-attached themselves to the rock surfaces. The specimen was exposed to toluene vapor with near-100% RH for 5 days. We locate the bacteria, toluene, and the toluene early metabolites on the rock surfaces via their spectral signature. We observed peak toluene and its early metabolites near the peak locations of *A. oxydans*, implying that the toluene was sorbed to the bacterial cells.

lites, benzyl alcohol ($\sim 1023\ cm^{-1}$) and catechol ($\sim 769\ cm^{-1}$), over the surface area of the rock sample. Fig. 11 shows the abundance of these compounds after 5 days of exposing the rock sample to 90 ppm toluene vapor at 100% RH. The location of the highest peaks of the chemical marker coincides with the toluene and metabolite peaks, implying that toluene sorbed to the bacteria cells. Fig. 12 shows the relative peak

Fig. 10. SEIRA spectra showing the transition from bacteria-containing to bacteria-free basalt surface along axis BB′ (see Fig. 7B). The biomarker peaks (at 1650 and 1550 cm^{-1}) are prominent in region A, decrease significantly in region B, and disappear in region C. The decrease of biomarker peaks in regions B and C coincides with a change of spectral features in regions E and F mostly caused by changes in mineralogy. Comparison with the confocal micrograph (Fig. 9) indicates that not all the indigenous bacteria fluoresce under simultaneous excitation at 488 and 510 nm.

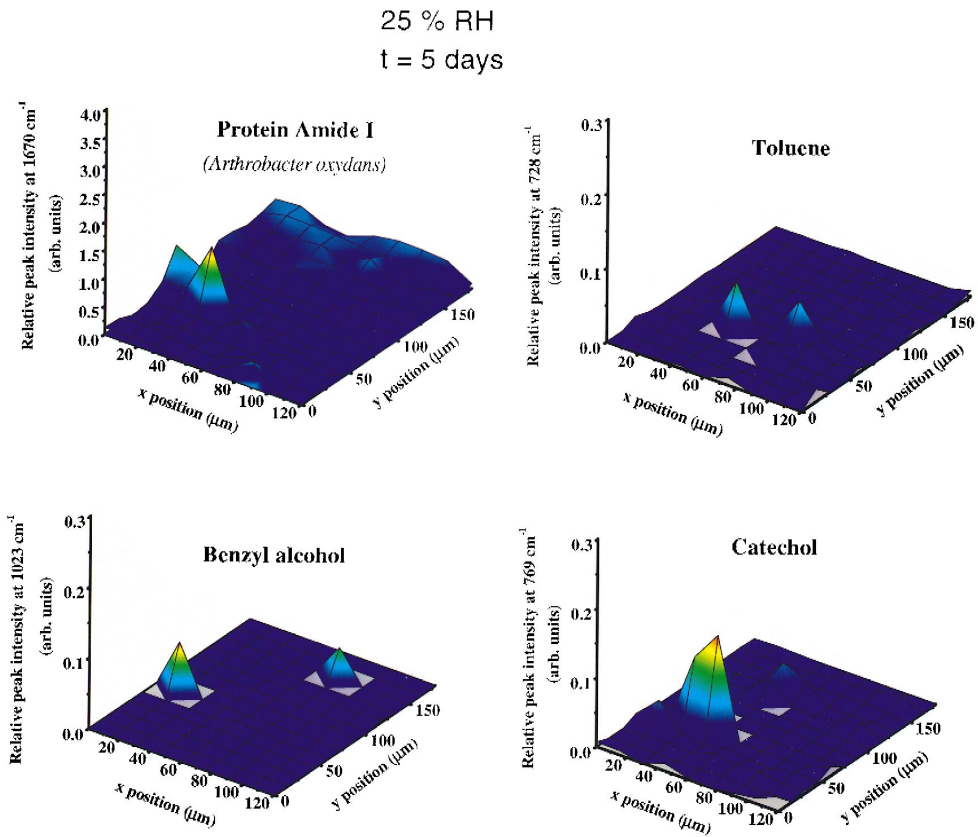

Fig. 12. The same specimen in Fig. 11 was returned to toluene vapor with 25% RH for 5 days. Biomass, sorbed toluene and the toluene early metabolites on the rock surface decreased significantly relative to the more moist conditions.

intensities after the same specimen was exposed to toluene vapor at 25% RH for 5 days. The large decrease in biomarker peaks relative to the conditions of 100% RH is accompanied by a decrease in presumably sorbed toluene, which may indicate a significant decrease in biomass at the lower RH conditions.

In a separate, complementary experiment, we observed that the same bacteria exposed to 23% RH air can be revived when the ambient air humidity is returned to 100% RH (Holman et al., 1997). The bacteria were incubated on an aluminized microscope slide that was coated with a thin film of basalt extract and monitored with FTIR while changing the RH from 100% to 23% and back to 100%. The spectra in Fig. 13 show that the biomarker peaks decreased significantly after 7 days of exposure to 23% RH air, and began to increase after 6 h of exposure to 100% RH air.

4.2.2. Geocosm experiments

Coupling between fluid flow and microbial activity arises from the likelihood that biological growth occurs in the path of the seepage water, and may alter the transport properties of the rock due to blockage or change in solid surface properties by biofilm

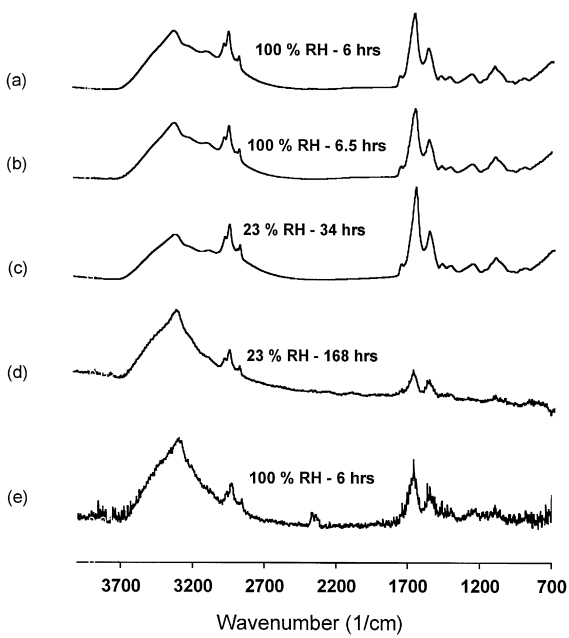

Fig. 13. FTIR spectra recorded from the Gram-negative basalt-inhabiting bacteria on an aluminized microscope slide coated with a thin film of basalt extract. The decline and subsequent increase in the biomarker peaks show that bacteria that have been exposed to dry air can be revived with exposure to 100% RH. (a) After 6 h of exposure to air at 100% RH; (b) 0.5 h later; (c) after reduction of humidity to 23% RH and 34 h exposure; (d) 134 h later; (e) after return to 100% RH and 6 h exposure.

formation and change in liquid surface tension. The presence of residual NAPL will further alter the patterns of microbial activity and subsequent water seepage.

In ''open'' geocosm experiments, we introduce water into a fracture that is assembled from one piece of the rock, mated to the transparent epoxy replica of the second side of the fracture. These experiments incorporate some aspects of natural conditions, while providing direct visual observation of flow dynamics. In the experiment reported here, the rock was a natural fracture in dense basalt from an outcrop at Box Canyon, an uncontaminated site adjacent to the INEEL. The replica and rock were sterilized, then the rock fracture surface was sprayed with a mixed culture of microorganisms derived from the defensible samples to an estimated coverage of 7×10^7 cells/cm^2.

The rock–replica assembly, inclined at 20° from the horizontal, was enclosed in a box with a glass cover, in which ambient air was maintained at 100% RH (Fig. 14). Seepage water was obtained from a rock extract solution, in order to reproduce the chemical composition of infiltrating water that equilibrates with the host rock during percolation. Chemical analysis showed that major nutrients in the rock-extract water included nitrate, magnesium, iron, potassium and sulfate; no phosphate was detected. To ensure that we would observe the effects of biological activity on flow in this first experiment, readily degradable glucose was added at a concentration of 10 mg/l as a carbon source. The rock extract with the glucose had approximately 130 mg/l non-volatile organic carbon (BC Laboratories, 1998). The cause of the high natural organic carbon (approximately 120 mg/l) is not known. Fluorescein ($C_{20}H_{10}O_5Na_2$) was added to the water at 200 mg/l to permit flow visualization by illumination with near-UV light, which may or may not have been an available carbon source. The seepage water

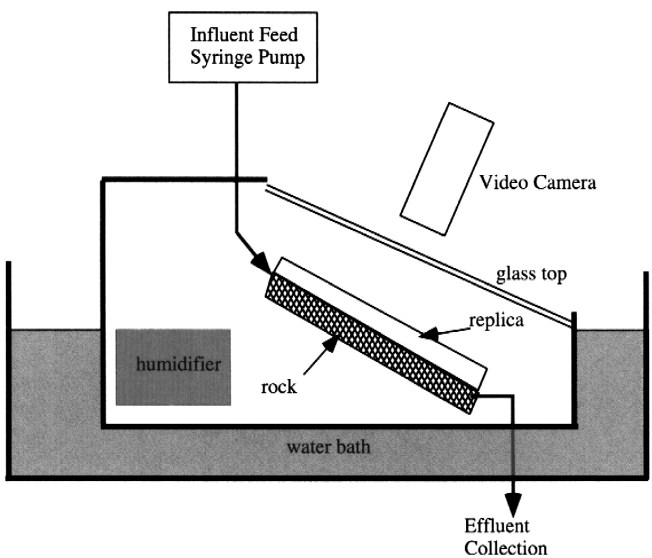

Fig. 14. Open geocosm experimental apparatus.

was sterilized by passing it through a sterile 0.2-μm filter. A syringe pump delivered the solution at a constant flow rate of 0.33 ml/h. Strips of glass-fiber filter paper were placed along the top and bottom of the fracture for liquid distribution and collection. Effluent was collected below the fracture outlet and was periodically extracted by syringe for sample analysis.

Indicators of biological activity within the fracture during seepage included an increase in the counts of colony-forming units (CFUs) in the effluent, and changes in surface tension and total dissolved solids of the effluent water compared to the influent water, and changes in seepage patterns over time. The fracture effluent was analyzed for bacteria counts by plating onto soil–rock extract agar.

Mass balance of the water delivered to the fracture and collected in the effluent indicated no measurable absorption of water into the dense basalt matrix. Effluent counts were on the order of 10^7–10^8/ml, with an increasing trend during the experiment that appears to be inversely correlated with the surface tension of the effluent (Fig. 15). The agar plates showed the presence of a mixed culture, including organisms with a tendency to spread and of varied pigmentation. Identification of half of the 20 isolates from this experiment using FAME analysis showed that these were the same microorganisms identified in the core sample isolates from which the mixed culture was obtained. Effluent surface tension generally decreased over time, from initial values of 75–55 dynes/cm. The effluent pH values ranged from 7.3 to 8.3, exhibiting no clear trend with time, and electric conductivity of the effluent was about 50% greater than the influent, also showing no clear trend with time.

Seepage patterns shown in Fig. 16 exhibit features observed in the replica studies described earlier, such as channelized flow and capillary pools connected by thin rivulets. The flow channel was initially a single rivulet that extended along the length of the fracture and periodically snapped near the bottom of the fracture plane (Fig. 16a). After 1 week, a capillary pool formed in the channel path about one third the way down the fracture plane (Fig. 16b). This residual most likely formed from condensed water vapor that migrated into the flow channel from the edges of the fracture. One week later,

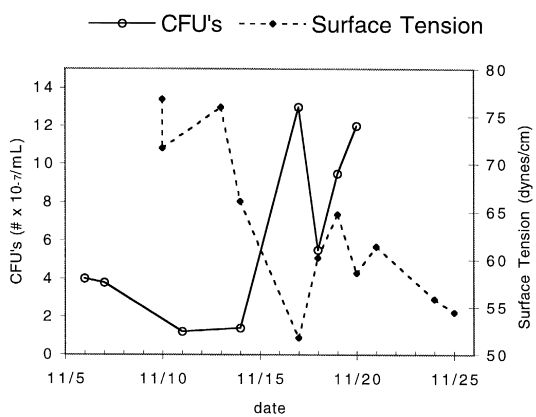

Fig. 15. CFUs and surface tension changes in rock–replica geocosm effluent.

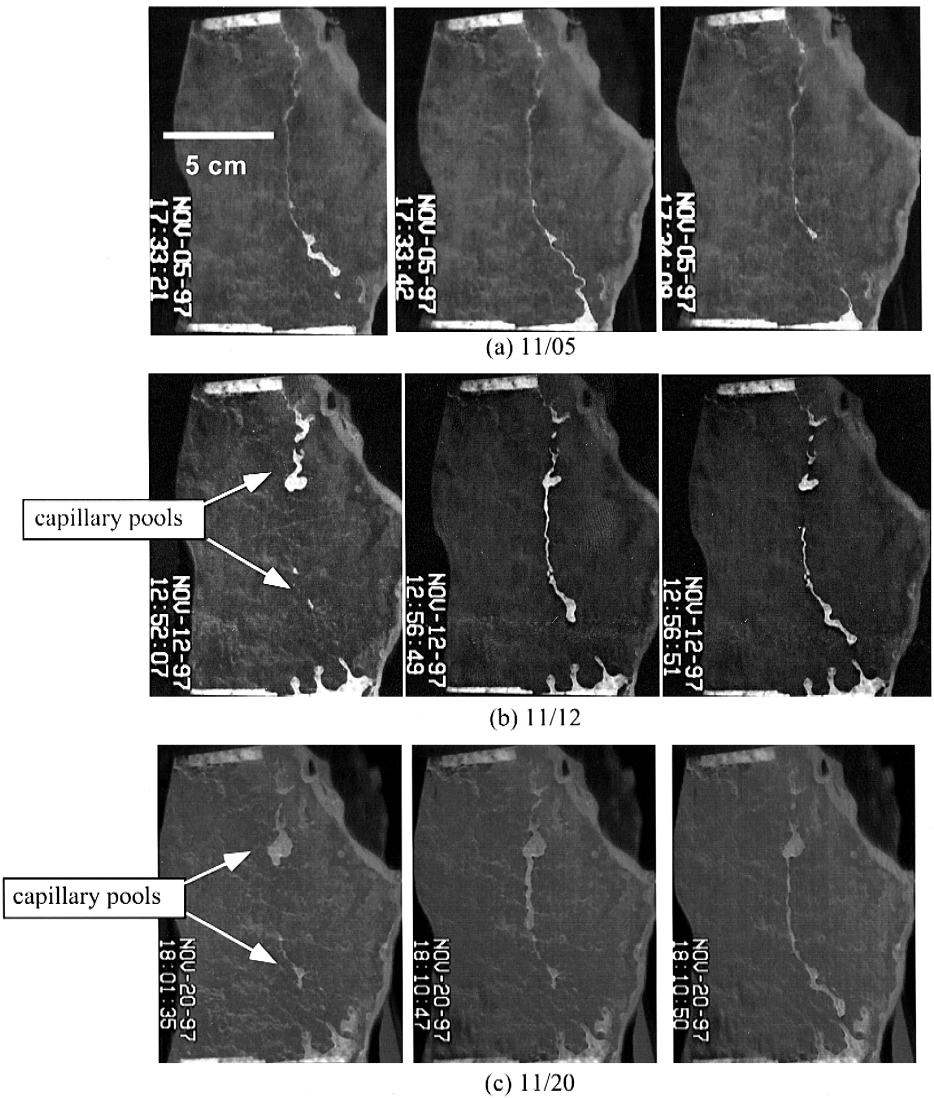

Fig. 16. Effect of biological growth on liquid seepage patterns. Images are of water seeping through the rock–replica open geocosm, where the rock fracture surface was innoculated with a mixed culture derived from defensible samples. Fluorescein was added to the water to promote visualization. Between 11/05 (a) and 11/12 (b), water vapor condensed in flow path creating ''capillary pools'', affecting flow behavior. The growth in the capillary pool in (c) 11/20 corresponds to the increase in effluent bacteria and decrease in surface tension shown in Fig. 15.

the fracture surface area covered by liquid residual increased (Fig. 16c). Since surface tension decreased and CFUs increased during this time (Fig. 15), the increased liquid saturation may be a result of biological activity. The presence of capillary pools in the

path of the flow channel had a significant effect on flow behavior. Cycles of filling and partial drainage of each capillary pool into the downstream pool prevented the formation of a continuous, connected flow channel.

5. Summary and conclusions

Deep fractured rock vadose zones in arid regions have been thought of as biologically inactive, due to dry conditions and minimal organic matter (Palumbo et al., 1994). However, bacteria are ubiquitous and have been found in such environments, albeit in low numbers (Colwell, 1989; Palumbo et al., 1994). Physical and numerical experiments indicate that water seepage in a fractured rock vadose zone is localized and intermittent. Nonetheless, adequate water to maintain the viability of bacteria is likely to exist in the vadose zone because RH will be near 100%. In addition, due to the layered structure of basalt flows, perched water can occur at sedimentary interbeds, with water flowing through fractures and rubble zones and imbibing into the high-storativity vesicular basalt.

Our studies have shown that a mixed culture of viable bacteria exists on the vesicle surfaces of defensible samples. This observation supports the existence of bacteria on fracture surfaces, even though defensible fracture samples cannot be obtained for confirmation. We hypothesize that the activity of these bacteria can be stimulated by contact with liquid water and organic contaminants. We further hypothesize that this activity will not only be localized along active seepage pathways, but will also occur in the presence of vapor-phase organic contaminants and water-saturated air.

NAPL organic contaminants migrate through the most permeable pathways, which, in the case of the fractured basalt vadose zone, are the fractures within the basalt flows and rubble zones between flows. The NAPL will pond at vertical discontinuities and the presence of residual water may redirect the NAPL to areas not contacted by the flowing water. However, much of the rock mass may be exposed to contamination due to the transfer of volatile and soluble organic compounds from the NAPL to the aqueous, vapor and solid phases, whereupon biological degradation of the organic contaminant may be a significant process in controlling its further migration.

Evaluating the biological activity in such systems and identifying the controlling factors require innovative laboratory studies that extend beyond traditional batch experiments. The development of high-resolution spectroscopic techniques to map bacteria, mineral and contaminant distributions provides potential for non-destructive monitoring of biological activity at the microscale. Larger-scale experiments can investigate the role of liquid seepage and distribution on biological activity.

We are currently applying this approach to test the effect of various environmental factors on biotransformation rates and to quantify potential isotopic shifts caused by biodegradation by measuring the abundance and stable isotopic composition of residual contaminants and of potential metabolic byproducts (e.g., CO_2). Quantifying any potential isotopic shifts caused by biodegradation of the contaminants is critical for developing the use of isotopic measurements for field monitoring and verification of bioremediation. The insights gained from this work should allow the design of tech-

niques to monitor and stimulate naturally occurring biological activity and control the spread of organic contaminants.

Acknowledgements

This work was supported by the Director, Office of Energy Research, Office of Health and Environmental Sciences, Biological and Environmental Research Program, of the U.S. Department of Energy under contract no. DE-AC03-76SF00098. We gratefully acknowledge Rick Colwell and Kirk Dooley of the INEEL for sample acquisition; Tamas Torok of the Center of Environmental Biotechnology (CEB) at LBNL for guidance and support in the microbiological work; and Terry Hazen and George Moridis of the Earth Sciences Division (ESD) at LBNL, David Lerner of the University of Sheffield and an anonymous reviewer for their review of this manuscript. Michael Martin, Wayne McKinney, Carol Hirschmugl of the Advanced Light Source at LBNL and Dale Perry of ESD collaborated in the FTIR development and Denise Schischnes and Steve Ruzin of the Center for Biological Imaging at University of California, Berkeley provided access and support for the confocal microscopy work.

References

Adamson, A.W., 1980. Physical Chemistry of Surfaces. 4th edn. Wiley, New York.

Amy, P.S., 1997. Microbial dormancy and survival in the subsurface. In: Amy, P.S., Haldeman, D.L. (Eds.), The Microbiology of the Terrestrial Deep Subsurface. CRC, Lewis Publishers, New York, pp. 185–204.

Balkwill, D.L., Boone, D.R., 1997. Identity and diversity of microorganisms cultured from subsurface environments. In: Amy, P.S., Haldeman, D.L. (Eds.), The Microbiology of the Terrestrial Deep Subsurface. CRC, Lewis Publishers, New York, pp. 105–118.

BC Laboratories, 1998. COC#980101, Laboratory no. 98-00153-1, Bakersfield, CA.

Colwell, F.S., Stormberg, G.J., Phelps, T.J., Birnbaum, S.A., McKinley, J., Rawson, S.A., Veverka, C., Goodwin, S., Long, P.E., Russell, B.F., Garland, T., Thompson, D., Skinner, P., Grover, S., 1992. Innovative techniques for collection of saturated and unsaturated subsurface basalts and sediments for microbiological characterization. J. Microbiol. Methods 15, 279–292.

Conant, B.H., Gillham, R.W., Mendoza, C.A., 1996. Vapor transport of trichloroethylene in the unsaturated zone: field and numerical modeling investigations. Water Resour. Res. 32 (1), 9–22.

Conrad, M.E., Daley, P.F., Fischer, M.F., Buchanan, B.B., Leighton, T., Kashgarian, M., 1997a. Combined ^{14}C and $\delta^{13}C$ monitoring of in situ biodegradation of petroleum hydrocarbons. Environ. Sci. Technol. 31, 1463–1469.

Conrad, M.E., DePaolo, D.J., Kennedy, B.M., Miller, E.C., 1997b. Carbon isotope evidence for degradation of mixed contaminants in the vadose zone. Geol. Soc. Am., Abstr. Prog. 26 (6), A186.

Costerson, J.W., 1995. Overview of microbial biofilms. J. Ind. Microbiol. 15, 137–140.

Demond, A.H., Lindner, A.S., 1993. Estimation of interfacial tension between organic liquids and water. Environ. Sci. Technol. 27 (12), 2318–2331.

Faybishenko, B., Doughty, C., Steiger, M., Long, J.C.S., Wood, T., Jacobsen, J., Lore, J., Zawislanski, P.T., 1999. Conceptual model of the geometry and physics of water flow in a fractured basalt vadose zone: Box Canyon site, Idaho. LBNL Report 42925. Lawrence Berkeley National Laboratory, Berkeley, CA 94720.

Geller, J.T., Su, G., Holman, H-Y., Conrad, M.E., Pruess, K., Hunter-Cevera, J.C., 1997. Processes controlling the migration and biodegradation of non-aqueous phase liquids (NAPLs) in the vadose zone: FY96 Annual Report. LBNL Report 39996, UC-400. Lawrence Berkeley National Laboratory, Berkeley, CA 94720.

Geller, J.T., Su, G., Holman, H-Y., Conrad, M.E., Pruess, K., Hunter-Cevera, J.C., 1998. Processes controlling the migration and biodegradation of non-aqueous phase liquids (NAPLs) within fractured rocks in the vadose zone. FY97 Annual Report, LBNL Report 41387. Lawrence Berkeley National Laboratory, Berkeley, CA 94720.

Geller, J.T., Su, G., Pruess, K., 1996. Preliminary studies of water seepage through rough-walled fractures. LBNL Report 38810. Lawrence Berkeley National Laboratory, Berkeley, CA 94720.

Gentier, S., 1986. Morphologie et comportement hydroméchanique d'une fracture naturelle dans un granite sous constrainte normale. Ph.D. Thesis, Univ. D' Orléans, France.

Glass, R.J., 1995. Quantitative visualization of entrapped phase dissolution within a horizontal flowing fracture. Geophys. Res. Lett. 22 (11), 1413–1416.

Haldeman, D.L., Amy, P.S., Ringelberg, D., White, D., 1993. Characterization of the microbiology within a 21-m^3 section of rock from the deep subsurface. Microb. Ecol. 26, 145–159.

Hoeppel, R.E., Hinchee, R.E., Arthur, M.F., 1991. Bioventing soils contaminated with petroleum hydrocarbons. J. Ind. Microbiol. 8, 141–146.

Holden, P.A., Hunt, J.R., Firestone, M.K., 1997. Toluene diffusion and reaction to unsaturated *Pseudomonas putida* biofilms. Biotechnol. Bioeng. 56 (6), 656–670.

Holman, H.-Y.N., Perry, D.L., Hunter-Cevera, J.C., 1997. Use of infrared microspectroscopy to assess effects of relative humidity on microbial population and their activity in fractured rocks. In: Gordon Conference on Applied Environmental Microbiology, August 17–22, 1997. .

Holman, H.-Y.N., Perry, D.L., Hunter-Cevera, J.C., 1998a. Surface-enhanced infrared absorption reflectance (SEIRA) microspectroscopy for bacteria localization on geologic material surfaces. J. Microbiol. Methods 34, 59–71.

Holman, H.-Y.N., Perry, D.L., Martin, M.C., Lamble, G.M., McKinney, W.R., Hunter-Cevera, J.C., 1999. Real time characterization of biogeochemical reduction of Cr(VI) on basalt surfaces by SR-FTIR imaging. Geomicrobiol. J. 16 (4), in press.

Holman, H.-Y.N., Perry, D.L., Martin, M.C., McKinney, W.R., 1998b. Applications of synchrotron infrared microspectroscopy to the study of inorganic–organic interactions at the bacterial–mineral interface. In: Application of Synchrotron Radiation Techniques to Materials Sciences. MRS Symp. Ser. 54, pp. 17–24.

Johnson, R.L., Kueper, B.H., 1996. Experimental studies of the movement of chlorinated solvent compounds and other DNAPLs in the vadose, capillary, and groundwater zones. In: Pankow, J.F., Cherry, J.A. (Eds.), Dense Chlorinated Solvents and other DNAPLs in Groundwater: History, Behavior and Remediation. Waterloo Press, Portland, OR, pp. 145–178.

Knutson, C.F., McCormick, K.A., Smith, R.P., Hackett, W.R., O'Brien, J.P., Crocker, J.C., 1990. FY89 Report: RWMC vadose Zone basalt characterization. Informal Report EGG-WM-8949. EG&G Idaho, Idaho Falls, ID 83415.

Kueper, B.H., McWhorter, D.B., 1996. Physics governing the migration of dense non-aqueous phase liquids (DNAPLs) in fractured media. In: Pankow, J.F., Cherry, J.A. (Eds.), Dense Chlorinated Solvents and other DNAPLs in Groundwater: History, Behavior and Remediation. Waterloo Press, Portland, OR, pp. 337–353.

Lodman, D., Dunstan, S., Downs, W., Sondrup, J., Miyasaki, D., Galloway, K., Izbicki, K., 1994. Treatability study Report for the organic contamination in the vadose zone, OU 7-08. EGG-ER-11121, Idaho National Engineering Laboratory, EG&G Idaho, Idaho Falls, ID 83415.

Long, J.C.S., Doughty, C., Faybishenko, B., Aydin, A., Freifeld, B., Grossenbacher, K.A., Holland, P., Horsman, J., Jacobsen, J.S., Johnson, T.M., Lee, K.H., Lore, J., Nihei, K., Peterson, Jr., J.E., Salve, R., Sisson, J.B., Thapa, B., Vasco, D., Williams, K.H., Wood, T.R., Zawislanski, P., 1995. Analog site for fractured rock characterization. Annual Report FY1995. LBL-38095, UC-600. Lawrence Berkeley National Laboratory, Berkeley, CA 94720.

Mackay, D., Shin, W.-Y., 1974. The aqueous solubility and air–water exchange characteristics of hydrocarbons under environmental conditions. In: Chemistry and Physics of Aqueous Gas Solutions. American Society Testing Materials, Philadelphia, PA, pp. 104–108.

Marshall, K.C., 1985. Mechanisms of bacterial adhesion at solid–water interface. In: Savage, D.C., Fletcher, M. (Eds.), Bacterial Adhesion. Plenum, New York, pp. 133–161.

Mendoza, C.A., Johnson, R.L., Gillham, R.W., 1996. Vapor migration in the vadose zone. In: Pankow, J.F.,

Cherry, J.A. (Eds.), Dense Chlorinated Solvents and other DNAPLs in Groundwater: History, Behavior and Remediation. Waterloo Press, Portland, OR, pp. 179–201.
Mercer, J.W., Cohen, R.M., 1990. A review of immiscible fluids in the subsurface: properties, models, characterization and remediation. J. Contam. Hydrol. 6, 107–163.
National Research Council, 1994. Alternatives for Ground Water Cleanup. National Academy Press, Washington, DC.
Nicholl, M.J., Glass, R.J., Wheatcraft, S.W., 1994. Gravity-driven infiltration instability in initially dry non-horizontal fractures. Water Resour. Res. 30 (9), 2533–2546.
Palumbo, A.V., McCarthy, J.F., Parker, A., Pfiffner, S., Colwell, F.S., Phelps, T.J., 1994. Potential for microbial growth in arid subsurface sediments. Appl. Biochem. Biotechnol. 45/46, 823–834.
Parker, B., Cherry, L., Gillham, A., 1996. The effects of molecular diffusion on DNAPL behavior in fractured porous media. In: Pankow, F., Cherry, A. (Eds.), Dense Chlorinated Solvents and other DNAPLs in Groundwater: History, Behavior and Remediation. Waterloo Press, Portland, OR, pp. 355–393.
Parker, B.L., Gillham, R.W., Cherry, J.A., 1994. Diffusive disappearance of immiscible-phase organic liquids in fractured geologic media. Ground Water 32 (5), 805–820.
Persoff, P., Pruess, K., 1993. Flow visualization and relative permeability measurements in rough-walled fractures. In: Proceedings of the Fourth International High-Level Radioactive Waste Management Conference, Las Vegas, Nevada, April 26–30, 1993 2 American Society of Civil Engineers, New York, pp. 2007–2019.
Persoff, P., Pruess, K., 1995. Two-phase flow visualization and relative permeability measurement in natural rough-walled rock fractures. Water Resour. Res. 31 (5), 1173–1186.
Powers, S.E., Anckner, W.H., Seacord, T.F., 1996. The wettability of NAPL-contaminated sands. ASCE J. Environ. Eng. 122 (10), 889–896.
Pruess, K., 1998. On water seepage and fast preferential flow in heterogeneous, unsaturated rock fractures. J. Contam. Hydrol. 30 (3–4), 333–362.
Pruess, K., 1999. A mechanistic model for water seepage through thick unsaturated zones in fractured rocks of low matrix permeability. Water Resour. Res. 35 (4), 1039–1051.
Riddick, J.A., Bunger, W.B., 1970. Organic Solvents — Physical Properties and Methods of Purification. 3rd edn. Wiley-Interscience, New York, NY.
Roberts, J.R., Cherry, J.A., Schwartz, F.W., 1982. A case study of a chemical spill: polychlorinated biphenyls (PCBs): 1. History, distribution and surface translocation. Water Resour. Res. 18 (3), 525–534.
Rousseau, J.P., Kwicklis, E.M., Gillies, D.C., 1997. Hydrogeology of the unsaturated zone, north ramp area of the exploratory studies facility, Yucca Mountain, Nevada. U.S. Geol. Surv. Water Resour. Invest. Rep., Denver, CO.
Seely, G.E., Falta, R.W., Hunt, J.R., 1994. Buoyant advection of gases in unsaturated soil. J. Environ. Eng. 120 (5), 1230–1247.
Sorenson, Jr., K.S., Wylie, A.H., Wood, T.R., 1996. Test Area North hydrogeologic studies test plan operable unit 1-07B. Report No. INEL-96/0105. Idaho National Engineering Laboratory, Idaho Falls, ID.
Su, G., Geller, J.T., Pruess, K., Wen, F., 1999. Experimental studies of water seepage and intermittent flow in unsaturated, rough-walled fractures. Water Resour. Res. 35 (4), 1019–1037.
Tchobanoglous, G., Schroeder, E.D., 1987. Water Quality. Addison-Wesley Publishing, Reading, MA.
Whitehead, R.L., 1992. Geohydrologic framework of the Snake River Plain Regional Aquifer System, Idaho and Eastern Oregon. U.S. Geological Survey professional paper 1408-B, U.S. Department of the Interior. U.S. Geological Survey, Denver, CO.
Zheng, M., Kellogg, S.T., 1994. Analysis of bacterial populations in a basalt aquifer. Can. J. Microbiol. 40 (11), 944–954.